

Accepted Manuscript

Research paper

New mononuclear dioxidomolybdenum(VI) complexes with hydrazone ligands: synthesis, crystal structures and catalytic performance

Cong Wang, Na Xing, Wenjing Feng, Sihan Guo, Mingyang Liu, Yue Xu, Zhonglu You

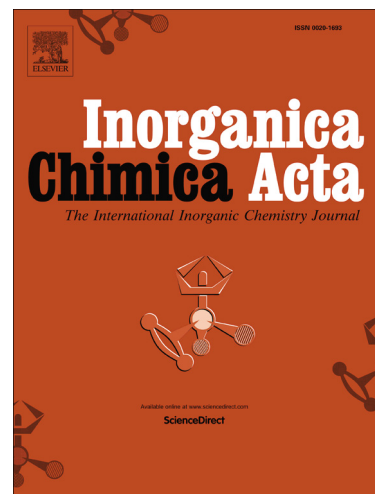
PII: S0020-1693(18)31273-8
DOI: <https://doi.org/10.1016/j.ica.2018.11.020>
Reference: ICA 18635

To appear in: *Inorganica Chimica Acta*

Received Date: 16 August 2018
Revised Date: 15 November 2018
Accepted Date: 16 November 2018

Please cite this article as: C. Wang, N. Xing, W. Feng, S. Guo, M. Liu, Y. Xu, Z. You, New mononuclear dioxidomolybdenum(VI) complexes with hydrazone ligands: synthesis, crystal structures and catalytic performance, *Inorganica Chimica Acta* (2018), doi: <https://doi.org/10.1016/j.ica.2018.11.020>

This is a PDF file of an unedited manuscript that has been accepted for publication. As a service to our customers we are providing this early version of the manuscript. The manuscript will undergo copyediting, typesetting, and review of the resulting proof before it is published in its final form. Please note that during the production process errors may be discovered which could affect the content, and all legal disclaimers that apply to the journal pertain.



New mononuclear dioxidomolybdenum(VI) complexes with hydrazone ligands: synthesis, crystal structures and catalytic performance

Cong Wang, Na Xing*, Wenjing Feng, Sihan Guo, Mingyang Liu, Yue Xu and Zhonglu You*

College of Chemistry and Chemical Engineering, Liaoning Normal University, Dalian 116029, P. R. China

Corresponding author. E-mail address: scarlet_na@163.com (N. Xing)
youzhonglu@163.com (Z. You)

Abstract

Three new dioxomolybdenum (VI) complexes, $[\text{MoO}_2\text{L}^1(\text{MeOH})]$ (**1**), $[\text{MoO}_2\text{L}^2(\text{MeOH})]$ (**2**) and $[\text{MoO}_2\text{L}^3(\text{H}_2\text{O})]\cdot\text{EtOH}$ (**3**), where L^1 , L^2 and L^3 are the dianionic form of N' -(2-hydroxybenzylidene)-3-methylbenzohydrazide, 4-bromo- N' -(2-hydroxybenzylidene)benzohydrazide and 2-bromo- N' -(2-hydroxybenzylidene)benzohydrazide, respectively, have been prepared and characterized by IR, UV-Vis and NMR spectra, as well as single crystal X-ray diffraction. The Mo atoms in the complexes are in octahedral coordination, with the ONO donor set of the hydrazone ligands, O atoms of the solvents, and two oxo groups. Crystals of the complexes are stabilized by hydrogen bonds of types $\text{O}-\text{H}\cdots\text{N}$ and $\text{O}-\text{H}\cdots\text{O}$. Moreover, the catalytic properties of complexes **1-3** are compared in cyclohexane oxidation. It was found that sebacic acid and FeCl_3 could promote the catalytic activities of the complexes.

Keywords: Hydrazone; Molybdenum complex; Crystal structure; Catalytic oxidation; Cyclohexane

1. Introduction

The selective oxidation of hydrocarbons is an important research object in the world [1-5]. Catalytic oxidation of cyclohexane (Cy) is a representative one, for its products of cyclohexanol (CyOH), cyclohexanone (CyO), adipic acid, glutaric acid and so on, are all important industrial products [6]. Soluble cobalt salts and complexes

are often used as industrial catalysts for this reaction. However, it usually takes higher temperature and pressure to overcome the inertness of C-H bond in the hydrocarbons [7-13]. Therefore, research has been done to improve the conditions of Cy reaction in industrial production [14]. For example, Sankar et al. reported that they used CoAlPO-11 as catalysis to Cy oxidation in air. The conversion of Cy could reach up to 16.1% at 403 K (130 °C) under 1.5 MPa [15]. Huang et al. also gave a similar condition that was realized on zinc oxide supported iron porphyrin at 423 K (150 °C) under 0.7 MPa [16]. Song et al. observed that the Al-Cu-Co catalyst was applied to Cy oxidation, and the selectivity of CyO reached 58.7% at 413 K (140 °C) under 0.5 MPa [17]. However, it is still a goal for catalytic oxidation of Cy at lower temperature below the boiling point of Cy (80.7 °C) to receive more reaction selective control and relieve the hazard [18].

In recent years, the main research has been focusing on metal salts beside Co, such as iron, copper, manganese and their complexes as catalysts [6, 19-21]. Wang et al. revealed that the total selectivity of the products (adipic acid+CyOH+CyO) reached to 79.7% in Cy oxidation with utilizing manganese porphyrins as catalyst and PhCOOH as co-catalyst [6]. Lindhorst et al. showed that the highest TON value of products was 317.3 when molecular iron complexes were used as catalysts and H₂O₂ as oxidant in alkane oxidation [21]. Li et al. reported that the yield of the product could reach to 46.2% with a porphyrinic MOF, PCN-222(Fe)-F7 as catalyst in the catalytic oxidation of Cy [22]. Among them, molybdenum complexes are particularly studied, for the molybdenum enzymes have been found to have excellent catalytic properties. They can regulate many physiological processes, such as hormone metabolism, carbon metabolism, nitrogen metabolism and active oxygen metabolism in plants [23-26].

Therefore, the catalytic activity of molybdenum complexes is worth being studied, especially these synthesized with molybdenum enzyme as template. The recent research has focused on the synthesis of Mo complexes with molybdenum oxidase, such as nitrate reductase, sulfite oxidase and xanthine oxidase that all contain MoO₂²⁺ group [27]. Biswal et al. showed that the dioxidomolybdenum (VI) complex [MoO₂L]₂•THF with an ONO donor ligand L (H₂L= 2-aminobenzoylhydrazone of

benzoylacetone) had a very good catalytic activity for the styrene oxidation (TOF= 4900 h⁻¹) [28]. Bagherzadeh et al. displayed that the complex containing MoO₂²⁺ and salicylidene 2-picoloyl hydrazone ligand had an excellent performance (the selectivity of epoxides are all 66 % above) in the epoxidation of seven olefins [29]. Gomes et al. reported that the selectivity of the acetalisation of benzaldehyde with ethanol at 55 °C was 100% at 10 min when complex [MoO₂Cl₂(L)] with L= 4,4'-di-*tert*-butyl-2,2'-bipyridine was used as a catalyst [30]. To sum up, it indicates that the complexes with MoO₂²⁺ as active site would have potential catalytic activity.

On the other hand, Schiff base complexes play important roles in many reactions due to their low cost, thermodynamic property stability, and high catalytic performance [31-33]. Hydrazone, a special kind of Schiff base, has more stable structure than common Schiff base in some aspects. Therefore, the synthesis of oxomolybdenum complexes with hydrazone and their catalytic activities in the oxidation of Cy are attracting much attention at present [34].

In this paper, three new dioxomolybdenum (VI) complexes, [MoO₂L¹(MeOH)] (**1**), [MoO₂L²(MeOH)] (**2**) and [MoO₂L³(H₂O)]·EtOH (**3**), where L¹, L² and L³ are the dianionic form of *N'*-(2-hydroxybenzylidene)-3-methylbenzohydrazide, 4-bromo-*N'*-(2-hydroxybenzylidene)benzohydrazide and 2-bromo-*N'*-(2-hydroxybenzylidene)benzohydrazide, respectively, have been prepared and structurally characterized. Their catalytic properties are also studied. By adjusting the temperature of the reaction, altering the solvent of the reaction, changing the amount of the reaction catalyst and the acid auxiliary, the optimum reaction conditions are found. Then, the effects of adding mixed acids on the reaction are explored. At last, the activity of the three complexes is compared.

2. Experimental

2.1. Materials and methods

Salicylaldehyde, 3-methylbenzohydrazide, 4-bromobenzohydrazide, and 2-bromobenzohydrazide were purchased from Sigma-Aldrich company. All other chemicals and solvents with AR grade were obtained from Xiya Reagent Co. Ltd. Elemental analyses were performed on a Perkin-Elmer 240C elemental analyzer. IR spectra were recorded on a Jasco FT/IR-4000 spectrometer as KBr pellets in the

4000–400 cm^{-1} region. UV-Vis spectra were recorded on a Perkin-Elmer Lambda 35 spectrometer. NMR spectra were recorded on a Bruker 500 MHz instrument. Single crystal structures were determined by a Bruker D8 Venture CCD area diffractometer. The 30% aqueous solution of H_2O_2 as a primary oxidant is used in Cy reactions. The Cy, CyOH and CyO are analyzed by GC-9790 series gas chromatograph that equips a FID detector and a capillary column. The carrier gas is nitrogen.

2.2. Synthesis of the complexes

Synthetic procedure

Salicylaldehyde (1.21 g, 0.01 mol) was diluted by 30 mL methanol (complex **1** and **2**) or ethanol (complex **3**), to which was added 3-methylbenzohydrazide (complex **1**, 1.50 g, 0.01 mol), 4-bromobenzohydrazide (complex **2**, 2.15 g, 0.01 mol) or 2-bromobenzohydrazide (complex **3**, 2.15 g, 0.01 mol). The mixtures were magnetic stirred for 30 min at room temperature to give colorless solution. Then, methanol or ethanol solution (30 mL) of $\text{MoO}_2(\text{acac})_2$ (3.30 g, 0.01 mol) was added to the above solution. The final mixtures were further stirred for 30 min at room temperature, to give orange solution. Single crystals of the complexes were obtained by slow evaporation of the solution in air for a period of a week.

Spectroscopic data

The complex **1**: The yield is 0.27 g (67%). IR data (KBr, cm^{-1}): 3447w, 1605s, 1553m, 1516m, 1477w, 1443m, 1385w, 1346m, 1269m, 1225w, 1124w, 1020w, 949m, 904s, 860m, 814w, 760m, 723w, 685w, 609m, 523w. UV-Vis data [methanol, λ/nm]: 205, 259, 298, 389. Anal. Calcd for $\text{C}_{16}\text{H}_{16}\text{MoN}_2\text{O}_5$: C, 46.6; H, 3.9; N, 6.8. Found: C, 46.7; H, 4.0; N, 6.7%.

The complex **2**: The yield is 0.35 g (73%). IR data (KBr, cm^{-1}): 3449w, 1610s, 1558m, 1528w, 1445m, 1393m, 1358m, 1269w, 1163s, 1074s, 951s, 860s, 750w, 677w, 548s, 523s. UV-Vis data [methanol, λ/nm]: 205, 268, 312, 393. Anal. Calcd for $\text{C}_{15}\text{H}_{13}\text{BrMoN}_2\text{O}_5$: C, 45.4; H, 3.3; N, 7.0. Found: C, 45.2; H, 3.3; N, 7.1%.

The complex **3**: The yield is 0.25 g (49%). IR data (KBr, cm^{-1}): 3252w, 1607s, 1558m, 1516m, 1472w, 1441m, 1383w, 1355m, 1273m, 1159s, 1074s, 949s, 903m, 860s, 761w, 644w, 548s, 521s. UV-Vis data [methanol, λ/nm]: 205, 282, 292, 314,

380. Anal. Calcd for $C_{16}H_{17}BrMoN_2O_6$: C, 37.7; H, 3.4; N, 5.5. Found: C, 37.9; H, 3.3; N, 5.6%.

2.3. X-ray structure determination

Diffraction intensities for the complexes were collected at 298(2) K using a Bruker D8 Venture diffractometer with $MoK\alpha$ radiation ($\lambda = 0.71073 \text{ \AA}$). The collected data were reduced with SAINT [35], and multi-scan absorption correction was performed using SADABS [36]. Structures of the complexes were solved by direct methods and refined against F^2 by full-matrix least-squares method using SHELXTL [37]. All of the non-hydrogen atoms were refined anisotropically. The hydrogen atoms of the methanol and water ligands were located from difference Fourier maps and refined isotropically, with O–H and H...H distances restrained to 0.85(1) and 1.37(2) \AA , respectively. The remaining hydrogen atoms were placed in calculated positions and constrained to ride on their parent atoms. Crystallographic data for the complexes are summarized in **Table 1**. Selected bond lengths and angles are given in **Table 2**.

Table 1. Crystal data for complexes.

	1	2	3
Formula	$C_{16}H_{16}MoN_2O_5$	$C_{15}H_{13}BrMoN_2O_5$	$C_{16}H_{17}BrMoN_2O_6$
FW	412.2	477.1	509.2
Crystal shape/colour	block/orange	block/orange	block/orange
Crystal system	Triclinic	Monoclinic	Triclinic
Space group	$P-1$	$P2_1/c$	$P-1$
a (\AA)	7.844(1)	12.218(1)	8.007(2)
b (\AA)	9.922(2)	9.4756(9)	11.066(2)
c (\AA)	11.164(2)	14.867(2)	11.644(2)
α ($^\circ$)	85.289(2)	90	70.317(3)
β ($^\circ$)	73.854(2)	104.234(2)	85.220(3)
γ ($^\circ$)	76.412(2)	90	71.357(3)
V (\AA^3)	811.2(2)	1668.4(3)	920.1(3)
Z	2	4	2
λ ($MoK\alpha$) (\AA)	0.71073	0.71073	0.71073
T (K)	298(2)	298(2)	298(2)
μ ($MoK\alpha$) (cm^{-1})	0.837	3.208	2.919
Reflections	6023	9617	6824

Unique reflections	4034	3109	3416
Observed reflections	2920	2590	4564
$[I \geq 2\sigma(I)]$			
Parameters	221	221	243
Restraints	1	1	3
Goodness of fit on F^2	1.059	1.048	1.043
$R_1, wR_2 [I \geq 2\sigma(I)]$	0.0557, 0.1139	0.0346, 0.0939	0.0434, 0.1120
R_1, wR_2 (all data)	0.0888, 0.1340	0.0447, 0.0999	0.0661, 0.1256

Table 2. Selected bond lengths (Å) and angles (°) for the complexes.

1			
Bond lengths			
Mo1–O1	1.918(4)	Mo1–O2	2.004(3)
Mo1–O3	1.695(4)	Mo1–O4	1.694(4)
Mo1–O5	2.384(4)	Mo1–N1	2.246(4)
Bond angles			
O4–Mo1–O3	107.2(2)	O4–Mo1–O1	102.54(17)
O3–Mo1–O1	98.34(19)	O4–Mo1–O2	97.29(16)
O3–Mo1–O2	97.32(18)	O1–Mo1–O2	149.73(15)
O4–Mo1–N1	155.59(17)	O3–Mo1–N1	95.78(18)
O1–Mo1–N1	81.49(15)	O2–Mo1–N1	71.27(14)
O4–Mo1–O5	81.78(16)	O3–Mo1–O5	170.60(16)
O1–Mo1–O5	81.88(16)	O2–Mo1–O5	78.56(14)
N1–Mo1–O5	74.92(13)		
2			
Bond lengths			
Mo1–O1	1.929(2)	Mo1–O2	2.010(2)
Mo1–O3	2.342(3)	Mo1–O4	1.697(3)
Mo1–O5	1.692(2)	Mo1–N1	2.238(3)
Bond angles			

O5–Mo1–O4	105.81(14)	O5–Mo1–O1	103.41(12)
O4–Mo1–O1	99.76(13)	O5–Mo1–O2	97.53(11)
O4–Mo1–O2	97.11(13)	O1–Mo1–O2	148.25(10)
O5–Mo1–N1	159.04(12)	O4–Mo1–N1	93.54(12)
O1–Mo1–N1	80.64(9)	O2–Mo1–N1	71.62(10)
O5–Mo1–O3	82.88(11)	O4–Mo1–O3	170.55(11)
O1–Mo1–O3	81.44(10)	O2–Mo1–O3	77.75(10)
N1–Mo1–O3	77.36(9)		
3			
Bond lengths			
Mo1–O1	1.921(3)	Mo1–O2	2.035(3)
Mo1–O3	1.702(3)	Mo1–O4	1.692(3)
Mo1–O5	2.269(3)	Mo1–N1	2.233(3)
Bond angles			
N1–Mo1–O5	76.55(11)	O1–Mo1–N1	81.31(12)
O1–Mo1–O2	150.55(13)	O1–Mo1–O5	82.81(13)
O2–Mo1–N1	71.25(12)	O2–Mo1–O5	80.64(13)
O3–Mo1–N1	95.31(14)	O3–Mo1–O1	97.79(16)
O3–Mo1–O2	95.24(15)	O3–Mo1–O5	171.68(14)
O4–Mo1–N1	157.87(14)	O4–Mo1–O1	104.27(14)
O4–Mo1–O2	97.66(14)	O4–Mo1–O3	104.94(16)
O4–Mo1–O5	82.86(13)		

Table 3. Distances (Å) and angles (°) involving hydrogen bonding of the complexes

<i>D–H···A</i>	<i>d(D–H)</i>	<i>d(H···A)</i>	<i>d(D···A)</i>	Angle(<i>D–H···A</i>)
1				
O5–H5···N2 ⁱ	0.85(1)	1.94(2)	2.770(5)	167(7)
2				
O3–H3···N2 ⁱⁱ	0.85(1)	1.94(1)	2.778(4)	173(6)
3				

O6–H6A···O3 ⁱⁱⁱ	0.82	2.01	2.798(5)	163(7)
O5–H5A···O6	0.85(1)	1.78(2)	2.611(5)	166(6)
O5–H5B···N2 ^{iv}	0.85(1)	1.98(2)	2.814(5)	167(5)

Symmetry codes: i) $1 - x, 1 - y, -z$; ii) $-x, -y, -z$; iii) $1 + x, y, z$; iv) $1 - x, 2 - y, 2 - z$.

2.4. Catalytic oxidation reaction

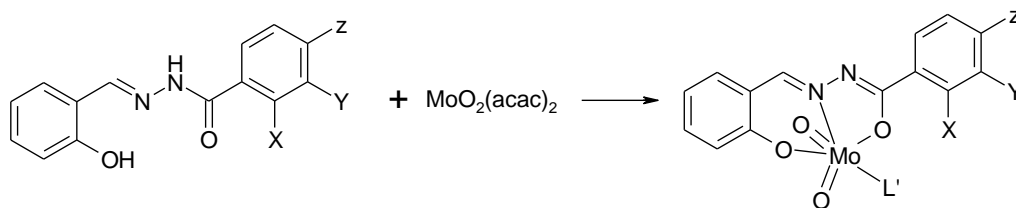
The Cy oxidation reactions are carried out in a glass flask with condenser pipes placed in a water bath with magnetic stirring. In a typical experiment, 0.0003 g of the catalysts (complex **1-3**) are dissolved in 3.00 mL of solvent. Then the required amount of Cy ($n_{\text{Cy}}: n_{\text{catalyst}} = 15000:1$) and HNO_3 ($n_{\text{HNO}_3}: n_{\text{catalyst}} = 2000:1$) are added according to this order. At last, a certain amount of 30% H_2O_2 ($n_{\text{H}_2\text{O}_2}: n_{\text{catalyst}} = 9000:1$) is added, that was stirred for 5 h at 80 °C.

For the products analysis, 0.03 g of methylbenzene (internal standard) and 1.5 mL of diethyl ether (to extract the substrate and the organic products from the reaction mixture) were added to 1.5 ml sample to detect the moles of CyOH and to calculate the conversion of Cy (a). 0.03 g of methylbenzene, 1.5 mL of diethyl ether and 0.3 g PPh_3 were added to 1.5 ml sample to detect the moles of CyO (b). The obtained mixtures were stirred for 10 min and then a sample (0.5 μL) was taken from the organic phase and analyzed by the internal standard method in the GC. The mole of CyOOH is calculated according to the equation of $[\text{CyOH}_{(b)} - \text{CyOH}_{(a)} + (\text{CyO}_{(a)} - \text{CyO}_{(b)})]$ and the TON values are the moles of products (CyOH / CyOOH or CyO) / mole of catalyst [38].

3. Results and discussion

3.1. Synthesis

The three complexes were synthesized by the reaction of $\text{MoO}_2(\text{acac})_2$ with the respective hydrazone compound in methanol for **1** and **2**, and in ethanol for **3**. For complexes **1** and **2**, the methanol solvent coordinated to the Mo atoms, while for complex **3**, the water solvent coordinated to the Mo atom.



1: X = Z = H, Y = Me, L' = MeOH; 2: X = Y = H, Z = Br, L' = MeOH; 3: X = Br, Y = Z = H, L' = H₂O

3.2. Crystal structure description of the complexes

The molecular structures of the complexes are shown in **Fig. 1-3**. In each complex, the Mo atom is coordinated with the phenolate O, imino N, and enalate O atoms of the hydrazone ligand, and one oxo group, forming an octahedral coordination. These define the equatorial plane, and with one oxo group and one solvent O atom (methanol for **1** and **2**, water for **3**) occupying the axial positions. The hydrazone ligands coordinate to the Mo atoms in meridional fashion forming five- and six-membered chelate rings with bite angles of 71.27(14)° and 81.49(15)° for **1**, 71.62(10)° and 80.64(9)° for **2**, and 71.25(12)° and 81.31(12)° for **3**. The hydrazone ligands are coordinated in enolate form, which are evident from the N2–C8 and O2–C8 bond lengths with values of 1.29-1.32 Å for the complexes. The Mo1–O1 and Mo1–N1 bond lengths in the complexes are comparable to each other, ranging from 1.918(4) to 1.929(2) Å and 2.246(4) to 2.238(3) Å, respectively. However, the Mo1–O2 bond lengths in **1** and **2** are much shorter than **3**, which might be caused by the effect of the substituent groups of the phenyl rings. The coordinate bond angles of the complexes are ranging from 71.2 to 107.2° for the *cis* angles and from 148.2 to 171.7° for the *trans* angles, which are comparable to those observed in similar molybdenum(VI) complexes [39-43].

In the crystal structure of **1** and **2**, adjacent two complex molecules are linked by two methanol molecules through intermolecular O–H⋯N hydrogen bonds to form a dimer (**Fig. 4** and **5**). In the crystal structure of **3**, adjacent two complex molecules are linked by two water molecules through intermolecular O–H⋯N hydrogen bonds to form a dimer. The dimers are further linked by ethanol molecules through O–H⋯O hydrogen bonds, to form chains along the *a* axis (**Fig. 6**).

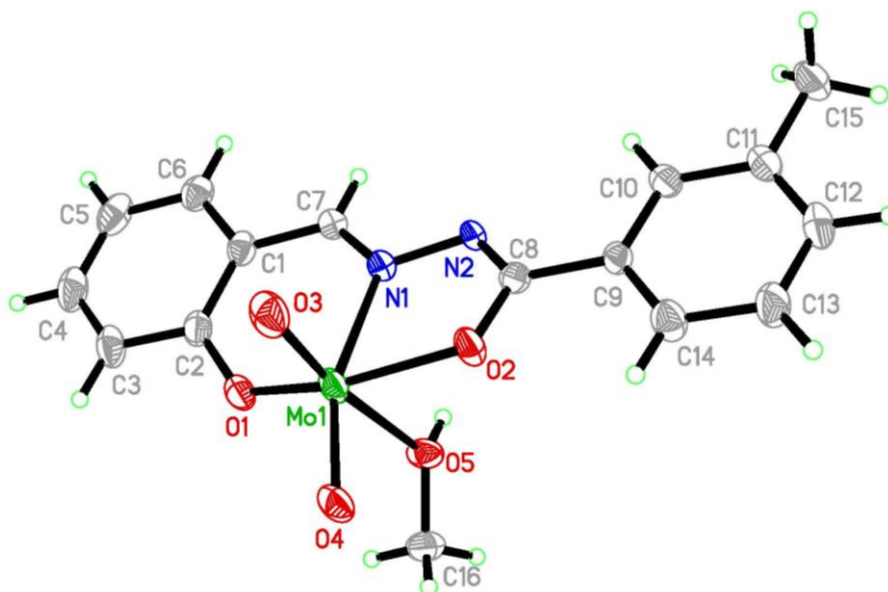


Fig. 1. Molecular structure of 1 with 30% probability thermal ellipsoids.

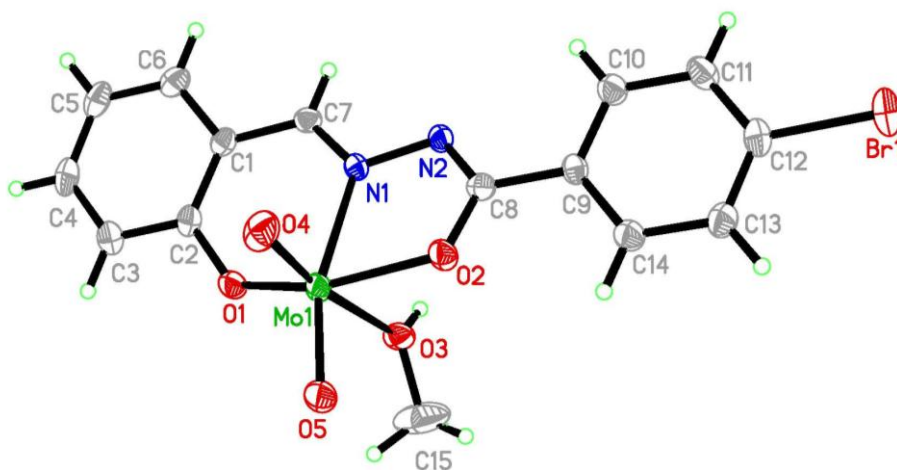


Fig. 2. Molecular structure of 2 with 30% probability thermal ellipsoids.

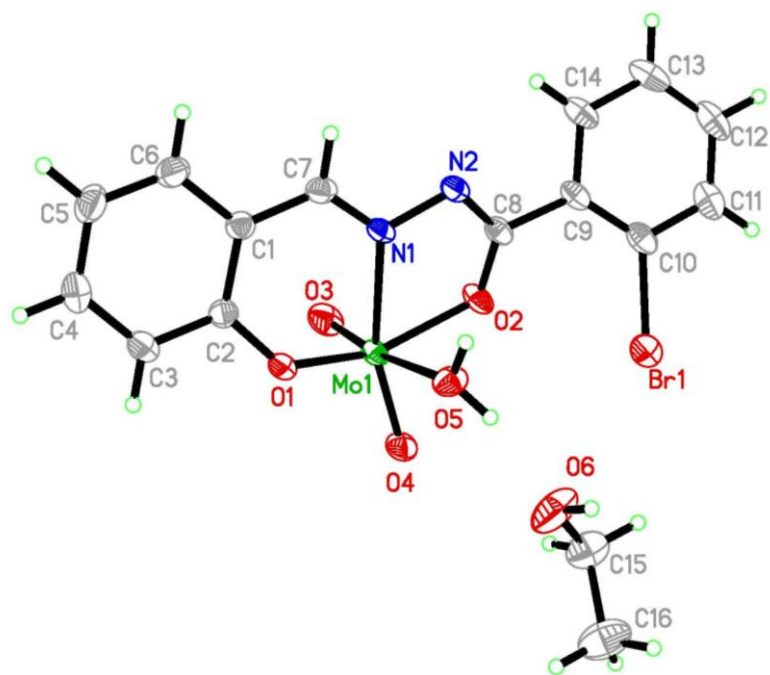


Fig. 3. Molecular structure of 3 with 30% probability thermal ellipsoids.

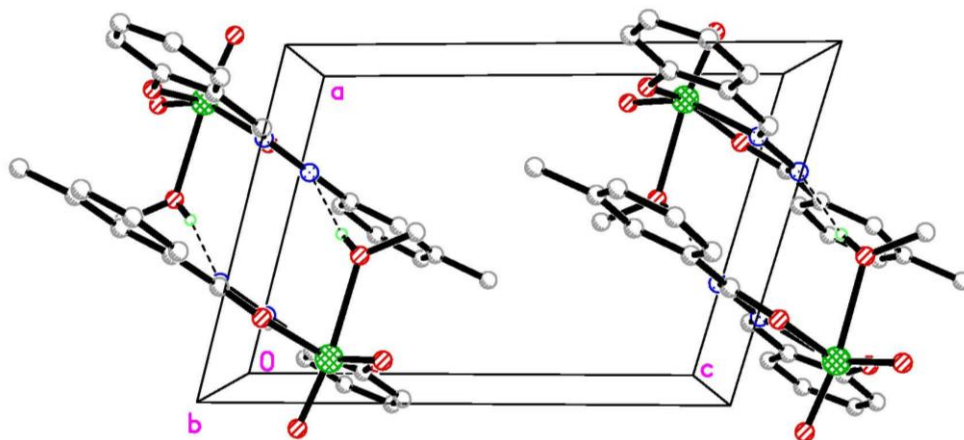


Fig. 4. Molecular packing of 1, viewed along the *b* axis. Hydrogen bonds are shown as dashed lines.

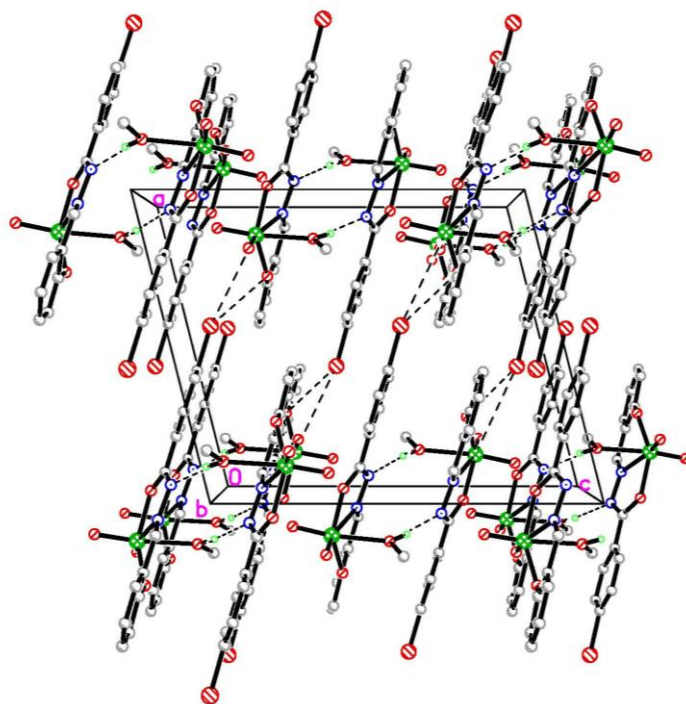


Fig. 5. Molecular packing of 2, viewed along the *b* axis. Hydrogen bonds are shown as dashed lines.

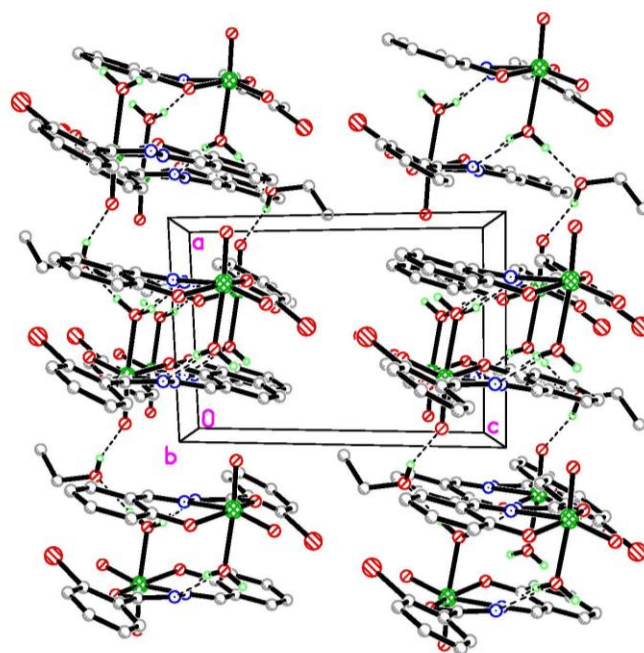


Fig. 6. Molecular packing of 3, viewed along the *b* axis. Hydrogen bonds are shown as dashed lines.

3.3. IR spectra

The infrared spectra of the complexes are shown in **Fig. S1-3**. The weak and broad vibration of O-H groups appears in the range of 3252–3449 cm^{-1} . The strong

vibrations observed at about 1607 cm^{-1} for the free hydrazones are assigned to the C=N groups in the spectra of complexes **1–3** [44-45]. As a result of the $\nu_{\text{asym}}(\text{O}=\text{Mo}=\text{O})$ and $\nu_{\text{sym}}(\text{O}=\text{Mo}=\text{O})$ modes, the complexes display two sharp bands in the $900\text{--}950\text{ cm}^{-1}$ region which are assigned to symmetric and anti-symmetric stretching vibrations of the *cis*-[MoO₂]²⁺ moiety [46-47]. The bands in the low wave $400\text{--}700\text{ cm}^{-1}$ may be assigned to the Mo-O and Mo-N bonds.

3.4. UV-vis spectra

The UV-Vis spectra of the complexes are shown in **Fig. S4-6**. All the complexes display intense absorption bands in the $380\text{--}393\text{ nm}$ region with $\epsilon_{\text{max}} = 2121\text{--}4638\text{ M}^{-1}\text{cm}^{-1}$ that are marked as L(p π) - Mo(d π) LMCT transitions involving the promotions of electrons from the filled HOMO of the ligand to the empty LUMO of molybdenum [48-49]. The bands at 298 nm , 312 nm and 314 nm ($\epsilon_{\text{max}} = 7193\text{--}13370\text{ M}^{-1}\text{cm}^{-1}$) are attributable to the $n\rightarrow\pi^*$ transitions of C=N group. These peaks are designated as transitions based on their extinction co-efficient values between electronic energy levels [46]. In addition, the peaks centered at 259 nm , 268 nm , 282 nm and 291 nm ($\epsilon_{\text{max}} = 9207\text{--}12858\text{ M}^{-1}\text{cm}^{-1}$) are attributed to the transition of the $\pi\rightarrow\pi^*$ in the hydrazone ligands of the complexes.

3.5 ¹H and ¹³C NMR spectra

The ¹H NMR spectra of the three complexes determined in *d*⁶-DMSO are shown in **Fig. 7-9** and their typical chemical shifts are presented in **Table S1**. In all complexes, the mono hydrogen on $-\text{CH}=\text{N}-$ has a significant peak which is attributed to $\delta = 8.95\text{--}8.94\text{ ppm}$. The Ar-H atoms in all the hydrazone ligands are assigned to $\delta = 7.93\text{--}6.95\text{ ppm}$. A singlet at $\delta = 2.39$ (3H) for **1**, a singlet at $\delta = 3.18$ (3H) for **1**, **2** and two singlets at $\delta = 3.44\text{ ppm}$ (2H), $\delta = 1.06\text{ ppm}$ (3H) for **3** are ascribed to the PhCH₃, Mo \cdots HOCH₃ and Mo \cdots HOCH₂CH₃ respectively. The absence of a signal from $-\text{OH}$ confirms an enolization prior to complexation, followed by a deprotonation during the complexation.

Table 4 provides ¹³C NMR spectral data of all compounds and **Fig. S7-9** reproduces their spectra. In all complexes, the signals at $\delta = 169\text{--}168\text{ ppm}$ are assignable to carbon bearing enolic oxygen. The absorption band at $\delta = 159\text{ ppm}$ is

attributed to carbons bearing azomethine nitrogen, and the carbons bearing phenolic oxygen are observed at $\delta = 155\text{--}157$ ppm. The carbons on the aromatic ring are assigned to $\delta = 138\text{--}118$ ppm. The carbon on coordinated methanol in complex **1** and **2** are assigned to $\delta = 48.6$ ppm. The carbon on coordinated ethanol in complex **3** are assigned to $\delta = 56.0$ ppm and $\delta = 18.5$ ppm. It was found that fewer numbers of aromatic carbon signals were observed in complex **2** due to the presence of symmetric axis, and the signal of terminal -CH_3 in complex **3** could be located at $\delta = 20.9$ ppm [50].

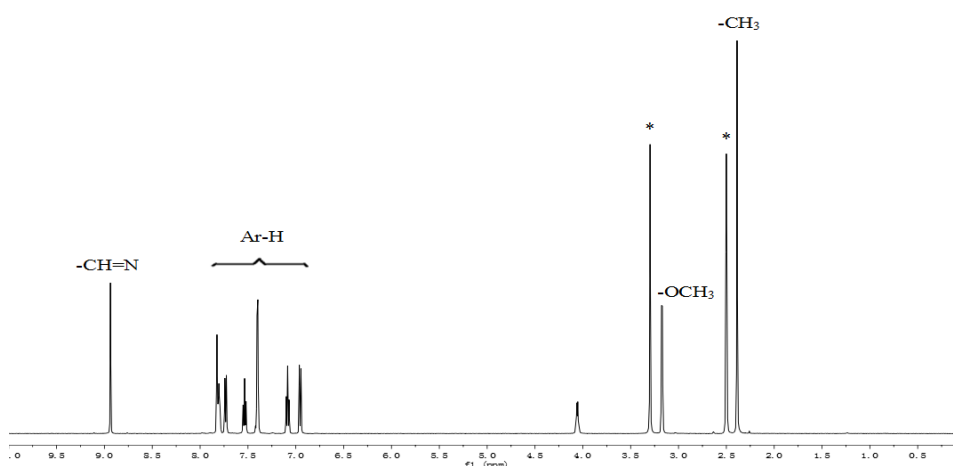


Fig. 7 ^1H NMR spectrum of complex **1**

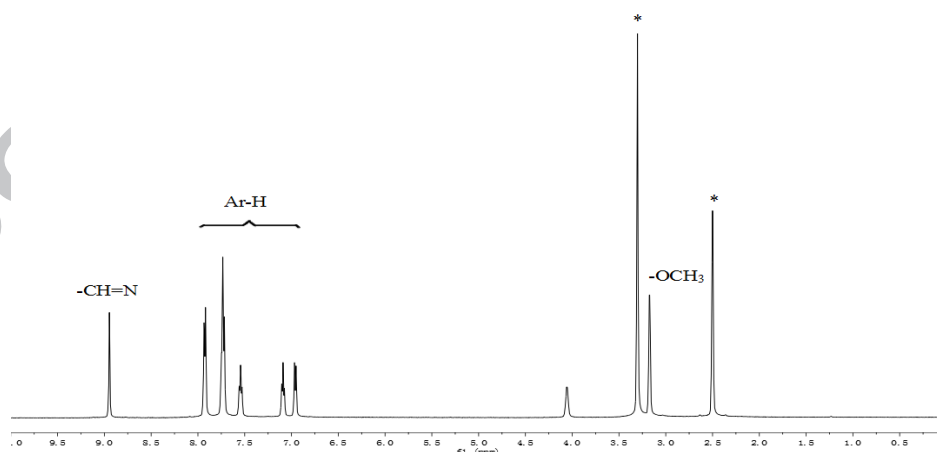
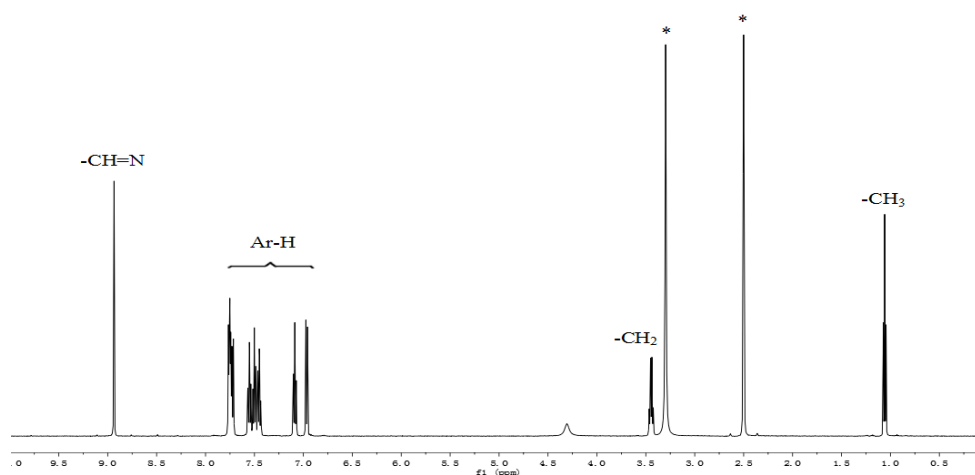


Fig. 8 ^1H NMR spectrum of complex **2**

Fig. 9 ^1H NMR spectrum of complex 3Table 4. ^{13}C NMR spectral data of complex 1–3.

Complex 1	168.79	155.85	159.36	138.06, 134.87, 134.22, 132.58, 129.88, 128.66, 128.35, 125.15, 121.53, 120.26, 118.52	20.89	48.57	\
Complex 2	167.91	156.32	159.38	135.04, 134.33, 131.88, 129.86, 129.20, 125.71, 121.64, 120.20, 118.54	\	48.57	\
Complex 3	169.48	157.00	159.49	135.15, 134.44, 133.80, 132.34, 132.18, 131.16, 127.70, 121.56, 120.69, 120.04, 118.60	\	\	56.00, 18.52

3.6 Thermal analysis

The thermal analyses of complexes **1**, **2** and **3** were carried out in order to study the thermal stability in air atmosphere (Figures S10-12). For complex **1**, the first weight loss of 6.82% at the temperature range from 88.9 °C to 280 °C is due to the loss of CH₃OH (calc. 7.76%). The second step can be caused by the weight loss of the ligand L¹, 60.9% with the temperature range from 280 °C to 581 °C (calc. 61.1%). For complex **2**, the first weight loss of 6.12% at the temperature ranges from 83.8 °C to 337 °C is due to the loss of CH₃OH (calc. 6.71%). The second step can be assigned to the weight loss of ligand L², 64.3% from 337 °C to 574 °C (calc. 66.4%). For complex **3**, the first weight loss of 4.25% at the temperature range from 97.6 °C to 118 °C is due to the loss of H₂O (calc. 3.53%). The second step can be attributed to the weight loss of ligand L³, 63.2% from 236 °C to 567 °C (calc. 62.3%). At this stage, the complexes turned to MoO₃. Then, with the increasing of the temperature, MoO₃ gradually sublimated [51].

3.7. Catalytic activity

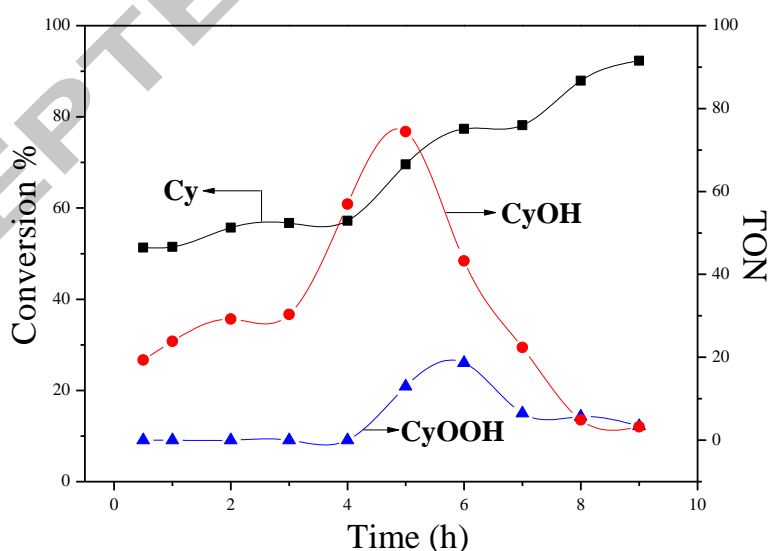


Fig. 10. The effect of time on Cy oxidation. Reaction conditions: Cy (0.7924 g, 9.434 mmol), complex **2** as catalyst (0.0003 g, 0.0006 mmol), H₂O₂ (0.6416 g, 5.661 mmol), HNO₃ (0.07924 g, 1.258 mmol), CH₃CN (3 mL), 40 °C.

The influence of reaction time on Cy oxidation is investigated by keeping the amounts of Cy (0.7924 g), complex **2** as catalyst (0.0003 g), H₂O₂ (0.6416 g) and

HNO₃ (0.07924 g) in CH₃CN (3 mL) at 40 °C, as shown in **Fig. 10**. The Cy conversion curve is continuously rising from 50 to 90% with the reaction time from 0.5 to 9 h, which is different from that of CyOH. The TON curve of CyOH is rising at first from 0 to 5 h, and reached the maximum value of 74.4. However, it decreased after that, which may be due to the further oxidation of CyOH to other by-products. What can be sure is that the CyOH or Cy cannot be oxidated further to CyO under this situation, for trace CyO (TON < 10) can be detected in all of our catalytic experiments, which is too small to be of significance for this discussion. On the other hand, the TON value curve of CyOOH has a similar shape with CyOH, and reaches the highest value of 18.7 at 6 h.

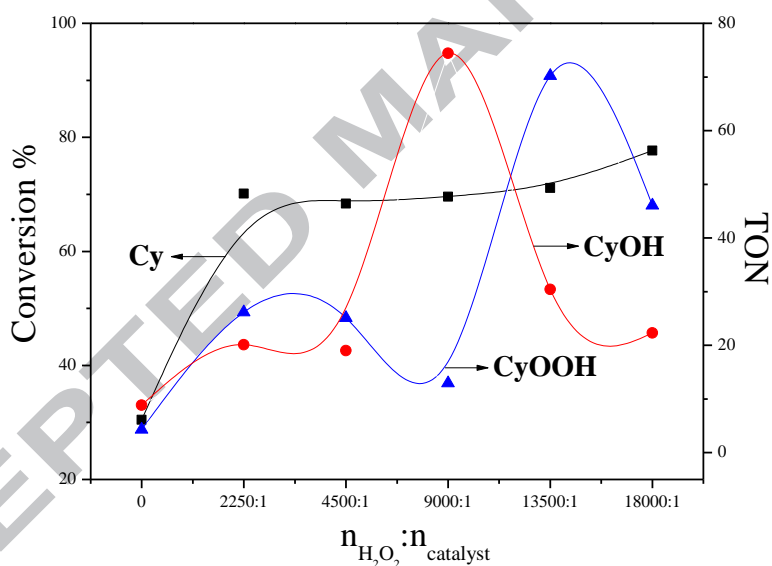


Fig. 11. The effect of the amount of H₂O₂ on Cy oxidation. Reaction conditions: Cy (0.7924 g, 9.434 mmol), complex **2** as catalyst (0.0003 g, 0.0006 mmol), HNO₃ (0.07924 g, 1.258 mmol), CH₃CN (3 mL), 40 °C, 5 h.

The effect of H₂O₂ on Cy oxidation over complex **2** is explored by keeping the amounts of Cy (0.7924 g), complex **2** (0.0003 g) and HNO₃ (0.07924 g) in CH₃CN (3 mL) at 40 °C for 5 h. As shown in **Fig. 11**, the curve of CyOH with a peak of 74.4 TON value at 9000:1 ratio and decreases after that. As for CyOOH, The TON value is only 13.0 at that ratio, which indicates that most of the CyOOH is converted into CyOH, since the TON value of CyOH is the highest. Although CyOOH has the highest TON value (70.2) at 13500:1 ratio, the TON of CyOH drops sharply to 30.4. This may be due to the hindrance of the water in the decomposition of CyOOH into

the target product. What also can be seen is that when there is no H_2O_2 in the system, a certain amount of products are still generated (CyOH TON= 8.83). It indicates that there exists another weak oxidant, HNO_3 . However, the Cy conversion without H_2O_2 is much lower than that with H_2O_2 , suggesting that H_2O_2 is the main oxidant in the reaction.

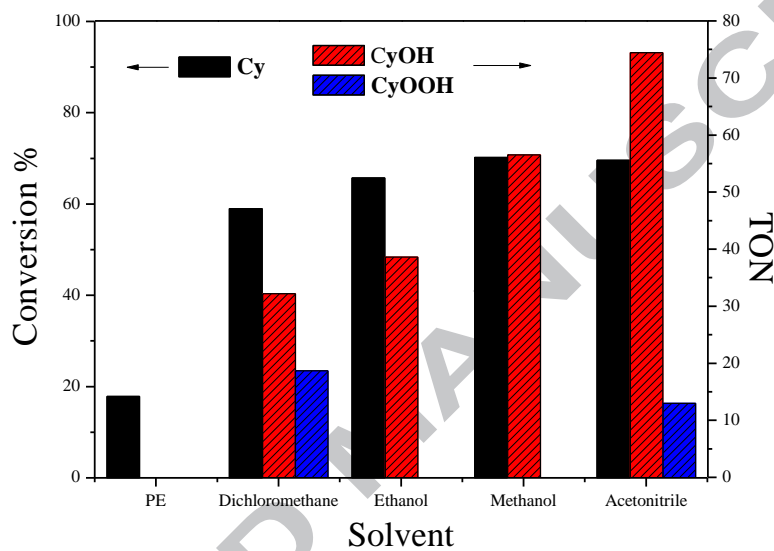


Fig. 12. The effect of the solvents on Cy oxidation. Reaction conditions: Cy (0.7924 g, 9.434 mmol), complex **2** as catalyst (0.0003 g, 0.0006 mmol), H_2O_2 (0.6416 g, 5.661 mmol), HNO_3 (0.07924 g, 1.258 mmol), Solvent (3 mL), 40 °C, 5 h.

A total of five different solvents (3 mL) CH_3CN , MeOH, EtOH, CH_2Cl_2 , and petroleum ether (PE) are evaluated in Cy oxidation, while complex **2** as catalyst (0.0003 g) at 40 °C and running for 5 h, in which the amount of Cy (0.7924 g), HNO_3 (0.07924 g), H_2O_2 (0.6416 g) were kept fixed, as shown in **Fig. 12**. It can be seen that the reaction in PE almost does not occur with the conversion rate of Cy being only 17.9 %. Though the reaction in CH_2Cl_2 yields a certain amount of CyOOH (TON= 18.7), the TON value of CyOH is only 32.2, indicating that CyOOH does not conductively transform to CyOH in CH_2Cl_2 . Compared to EtOH (TON= 38.6), the reaction of MeOH yields more CyOH (TON= 56.5). The highest $\text{TON}_{(\text{CyOH})}$, 74.4, is obtained in CH_3CN , and the CyOOH can also be detected. In summary, the order of $\text{TON}_{(\text{CyOH})}$ is $\text{PE} < \text{CH}_2\text{Cl}_2 < \text{EtOH} < \text{MeOH} < \text{CH}_3\text{CN}$, which is in good accordance with their dielectric constants (ϵ/ϵ_0): PE (~2) < CH_2Cl_2 (9.1) < EtOH (26.6) < MeOH

(32.7) < CH₃CN (37.5) [52].

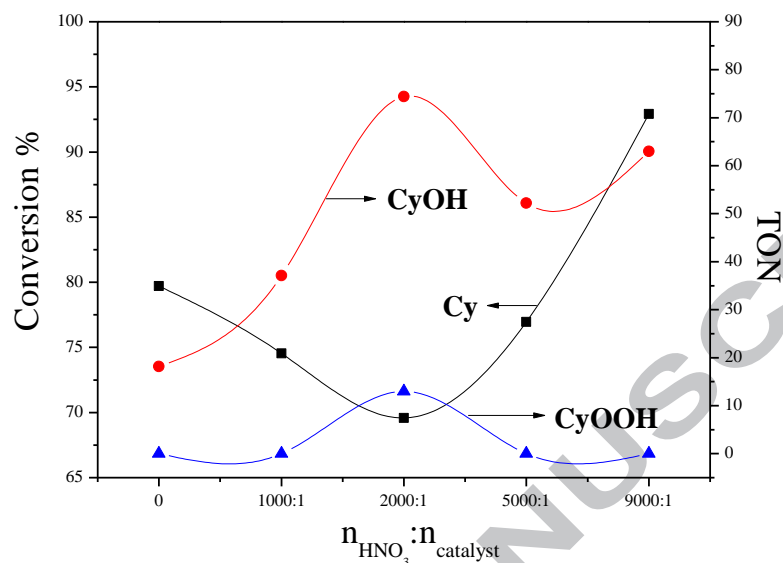


Fig. 13. The effect of the amount of HNO₃ on Cy oxidation. Reaction conditions: Cy (0.7924 g, 9.434 mmol), complex **2** as catalyst (0.0003 g, 0.0006 mmol), H₂O₂ (0.6416 g, 5.661 mmol), CH₃CN (3 mL), 40 °C, 5 h.

The effect of HNO₃ molar ratio on the catalytic activity of complex **2** for Cy oxidation is investigated, when the amount of Cy (0.7924 g), complex **2** (0.0003 g), H₂O₂ (0.6416 g), CH₃CN (3 mL) was set, at 40 °C and running for 5 h (shown in **Fig. 13**). It can be seen that with the increasing of HNO₃ mole ratio, the TON value of CyOH increases gradually, reaches the maximum value of 74.4, and decreases after that, which may be due to the deep oxidation of Cy to the by-product caused by a large amount of HNO₃. The TON value curve of CyOOH displays a similar shape as that of CyOH, with the highest TON 13.0 at the ratio of 2000:1 too. In particular, when there is no HNO₃, CyOH can still be found with the TON value is 18, indicating that H₂O₂ alone can oxidate Cy to CyOH directly.

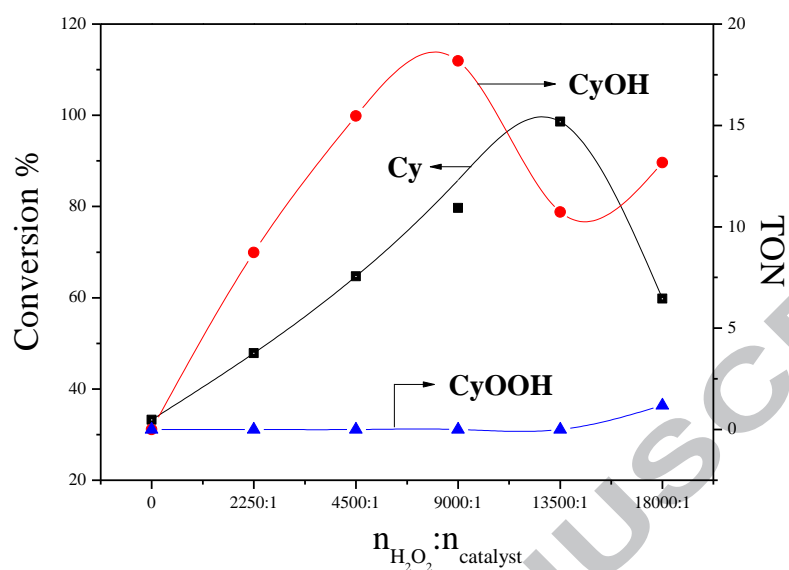


Fig. 14. The effect of the amount of H_2O_2 without HNO_3 on Cy oxidation. Reaction conditions: Cy (0.7924 g, 9.434 mmol), complex **2** as catalyst (0.0003 g, 0.0006 mmol), CH_3CN (3 mL), 40 °C, 5 h.

To discuss further the oxidation performance of H_2O_2 without acid, the amount of H_2O_2 is changed under the conditions of Cy (0.7924 g), complex **2** as catalyst (0.0003 g), CH_3CN (3 mL), 40 °C and 5 h, as shown in **Fig. 14**. It is intriguing that an obvious amount of CyOH with the largest TON value of 18.2 can be detected without acid but H_2O_2 . However, almost no CyOOH can be detected without HNO_3 considering the trend of $\text{TON}_{(\text{CyOOH})}$, which is quite different to the situation with HNO_3 . It seems that the addition of HNO_3 is the key to determine whether CyOOH can be produced. Therefore, it is speculated that when H_2O_2 is added alone, Cy is likely to be directly oxidated to CyOH. Otherwise, the reaction will go through the process of converting Cy to CyOOH first, and then to CyOH with HNO_3 .

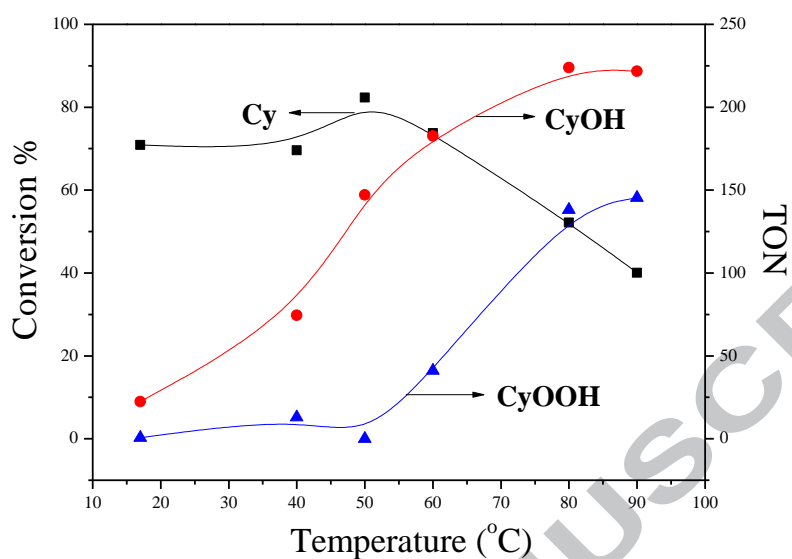


Fig. 15. The effect of the temperature on Cy oxidation. Reaction conditions: Cy (0.7924 g, 9.434 mmol), complex **2** as catalyst (0.0003 g, 0.0006 mmol), H₂O₂ (0.6416 g, 5.661 mmol), HNO₃ (0.07924 g, 1.258 mmol), CH₃CN (3 mL), 5 h.

The effect of reaction temperature for the Cy oxidation is detected under the conditions of Cy (0.7924 g), complex **2** (0.0003 g), H₂O₂ (0.6416 g), HNO₃ (0.07924 g), CH₃CN (3 mL) and 5 h catalyzed by complex **2**, and the results are shown in **Fig. 15**. As can be seen, the Cy conversion rate is almost unchanged, but begins to decline after 50 °C. However, more and more CyOH are generated (TON= 224) with the temperature rising to 80 °C. The reaction also produces much CyOOH (TON= 138) at 80 °C, which means that high temperature enhances the production of main products by promoting the production of intermediate products. Since the yield of the main product has not changed at 90 °C and a very small amount of CyO (TON= 9.04) has been generated, 80 °C is chosen as the best temperature considering the energy consumption.

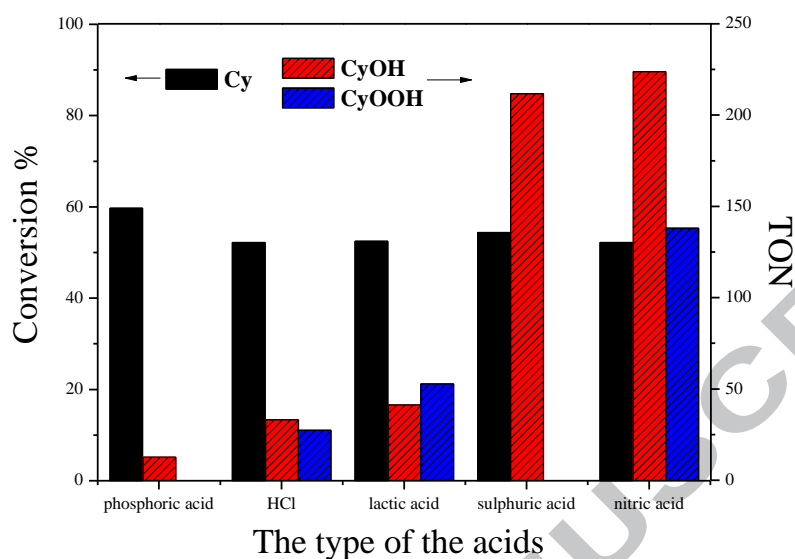


Fig. 16. The effect of the type of the acid on Cy oxidation. Reaction conditions: Cy (0.7924 g, 9.434 mmol), complex **2** as catalyst (0.0003 g, 0.0006 mmol), H_2O_2 (0.6416 g, 5.661 mmol), acid (1.258 mmol), CH_3CN (3 mL), 80 °C, 5 h.

As a common view, acid additives can enhance the catalyst's performance in oxidation. Tang et al. found that HCl was a good acid additive (TON= 76.1) when $\text{XPMo}_{12-n}\text{V}_n\text{O}_{40}$ was used as catalyst in MeCN and N_2 atmosphere [53]. Wu et al. detected that the TON value of CyO could reach to 83 when lactic acid was acting as acid additive promoted by ammonium paramolybdate, comparing to that in HNO_3 was only 41 [54]. Sutradhar et al. studied the performance of pyrazine carboxylic acid in the reaction of Cy oxidation in H_2SO_4 and found that the TON values of CyOH and CyO were higher than those in the traditional acid auxiliary TFA [55].

Herein, H_3PO_4 , HCl, lactic acid, H_2SO_4 and HNO_3 are chosen as acid additives under the condition of Cy (0.7924 g), complex **2** as catalyst (0.0003 g), H_2O_2 (0.6416 g), CH_3CN (3 mL), 80 °C and 5 h, as shown in **Fig. 16**. It is found that our catalyst has the lowest activity in H_3PO_4 , and is better in lactic acid and HCl. It produces the most CyOH and CyOOH in HNO_3 , with the TON values equal to 224 and 138, respectively. Though the TON of CyOH is slightly lower in H_2SO_4 , there is no intermediate product of CyOOH produced at all. In addition, a very small amount of CyO is detected in both HNO_3 (TON= 3.46) and H_2SO_4 (TON= 0.450).

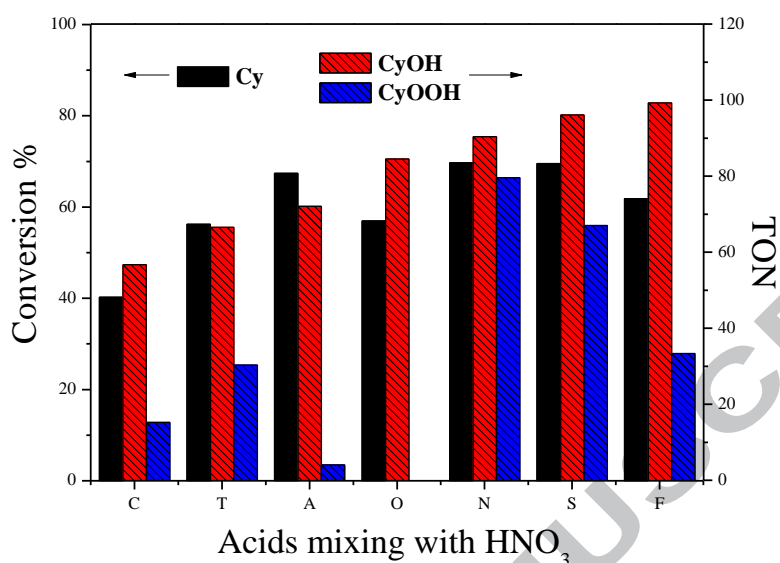


Fig. 17. The effect of acid mixture on Cy oxidation. Oxidation conditions: Cy (0.7924 g, 9.434 mmol), complex **2** as catalyst (0.0003 g, 0.0006 mmol), H_2O_2 (0.6416 g, 5.661 mmol), $\text{N} = \text{HNO}_3$ (0.0396 g, 0.6289 mmol), the molar ratio of acid to HNO_3 is 1:1 [C (citric acid), T (tartaric acid), A (AlCl_3), O (oxalate), S (Sebacic acid), F (FeCl_3)], CH_3CN (3 mL), 80°C , 5 h.

Moreover, other acids also have the ability to promote reactions. For instance, Pokutsa et al. showed that when oxalic acid was acid auxiliaries, the selectivity of CyOH and CyO is 22% and 44% and the total TON value of products is 944 [56]. Yiu et al. reported that when FeCl_3 was treated as acid auxiliary, the highest yield was at 91% when $[^n\text{Bu}_4\text{N}][\text{Os}(\text{N})\text{Cl}_4]$ was the catalyst [57]. Ho et al. observed that when AlCl_3 was the acid promoter, Cy was oxidized to chlorocyclohexane in $\text{CH}_3\text{COOH}-\text{CH}_2\text{Cl}_2$ with a yield of 24% with the barium ferrate as catalyst [58]. Du et al. also reported citric acid was used as acid additives, the conversion of Cy reached 93.3% and the selectivity of CyO reached 33.3% [59]. At the same time, we speculate that acid containing hydroxyl as an acid promoter may have a significant role in promoting the reaction due to the performance of lactic acid in the previous work [54], so tartaric acid may also have the possibility to enhance the reaction. It can be expected that the ability to enhance the reaction will be further enhanced by mixing the acid with HNO_3 . Herein, the effects of citric acid, tartaric acid, oxalate, sebacic acid, FeCl_3 and AlCl_3 on Cy oxidation is discussed under the condition of Cy (0.7924 g), complex **2** as catalyst (0.0003 g), H_2O_2 (0.6416 g), HNO_3 (0.0396 g), CH_3CN (3

mL), 80 °C, 5 h and the molar ratio of acid to HNO₃ is 1:1, as shown in **Fig. 17**. It is observed that the Cy conversion is not significantly affected by different acids, when the maximum value being 69.5% with sebacic acid was obtained. It indicates that the addition of acids have no special effect on the Cy conversion. Unfortunately, the TON values of CyOH and CyOOH decrease when citric acid, tartaric acid, AlCl₃, or oxalic acid is added to the system, indicating that these acids can not be acted as promoters with HNO₃ together. However, it increases when the acids are sebacic acid and FeCl₃, indicating that those two acids are potential good additives with HNO₃, though more study need to be done to clear out the reason. Moreover, FeCl₃ may have the potential to act as a catalyst alone considering it is a metal chloride and a type of Lewis acid. Therefore, we carry out a reaction with FeCl₃ under the same conditions without complex, and found that the Cy conversion is 55.1%, the TON value of CyOH 47.3 and no CyOOH is formation. Comparing with the catalytic performance of complex **2** + FeCl₃ together (Cy conversion= 61.8 %, CyOH TON= 99.3 and CyOOH TON= 33.4), we believe that FeCl₃ is acting as auxiliaries rather than catalyst in the reaction.

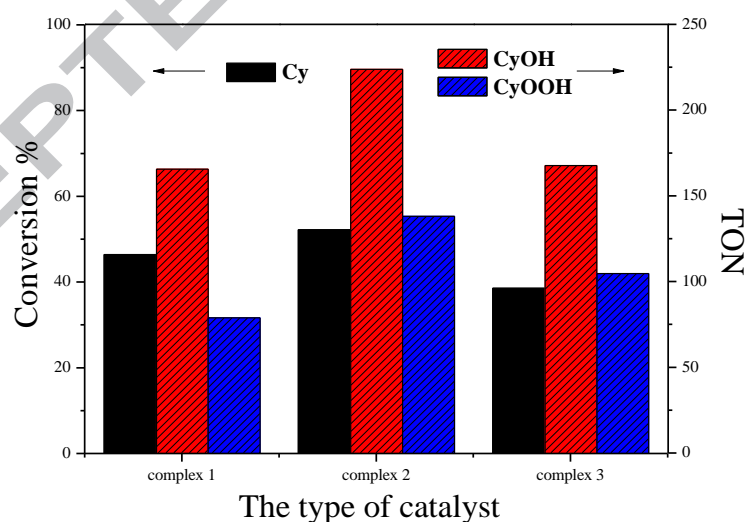


Fig. 18. The effect of the type of catalyst on Cy oxidation. Reaction conditions: Cy (0.7924 g, 9.434 mmol), complex **1**: [MoO₂L¹(MeOH)], complex **2**: [MoO₂L²(MeOH)] and complex **3**: [MoO₂L³(H₂O)]·EtOH as catalysts (0.0003 g), H₂O₂ (0.6416 g, 5.661 mmol), HNO₃ (0.07924 g, 1.258 mmol), CH₃CN (3 mL), 80 °C, 5 h.

Finally, the catalytic properties of our three different Mo complexes in the reaction of Cy (0.7924 g), H₂O₂ (0.6416 g), catalyst (0.0003 g), HNO₃ (0.07924 g), CH₃CN (3 mL), 80 °C and 5 h are compared, as shown in **Fig. 18**. It is observed that the catalytic

performance of complex **2** is the best: the Cy conversion (Conv.%= 52.2) and the TON value of its products (CyOH TON= 224, CyOOH TON= 138) are all the highest one in the three complexes. As we know, the stronger the electron withdrawing effect the ligand has, the easier it is to be close to the electrons of the center metal, which may have high catalytic performance by exposing more active metal center. As for the three complexes, the electron withdrawing effect of the bromine atoms in the complexes **2** and **3** are much stronger than that of methyl in complex **1**. Therefore, the catalytic activities is **2, 3** > **1**. On the other hand, if the bromine atoms at ligand terminals are adjacent to the coordination group, a certain aggregation of electrons at the coordination groups will be formed, which is not conducive to the exposure of the active sites to the central metal. That is why the catalytic activity of complex **2** is stronger than that of complex **3**.

Table 5. The comparison of $[\text{MoO}_2\text{L}^2(\text{MeOH})]$ (complex **2**) with other catalysts for Cy oxidation.

Entry	Catalyst	Time (h)	Temp. (°C)	n_{Catalyst} (mmol)	Reference	TON _(CyOH+CyO)
1	$[\text{MoO}_2\text{L}^2(\text{MeOH})]$	5	80	0.0006	This work	227
2 ^[a]	$[\text{MoO}_2(\text{L}^1)]$	9	70	0.0020	[60]	28
3 ^[b]	$[(\text{TpMoO}_2)_2(\mu\text{-O})\cdot\text{H}_2\text{O}]$	16	R.T.	$1.6\cdot 10^{-5}$	[61]	36
4 ^[c]	$[\text{Cu}_6(\text{H}_2\text{tea})_6\text{Fe}(\text{CN})_6]_n(\text{NO}_3)_{2n}\cdot 6n\text{H}_2\text{O}$	6	25	0.0010	[62]	110
5 ^[d]	$[\text{CuCo}^{\text{III}}\text{Co}^{\text{II}}_2(\text{MeDea})_3\text{Cl}_3(\text{CH}_3\text{OH})_{0.55}(\text{H}_2\text{O})_{0.45}(\text{H}_2\text{O})_{0.45}]$	5	20	0.0100	[63]	15
6 ^[e]	$[\text{FeCl}_2\{\eta^3\text{-HC}(\text{pz})_3\}]$ supported at CNT-Oxi-Na	6	R.T.	0.0099	[64]	78
7 ^[f]	$[\text{Fe}(\text{salhd})\text{Cl}]$	3	65	0.0500	[65]	13.6
8 ^[g]	$[\text{Fe}(\text{NCCN})(\text{MeCN})(\text{CN}^t\text{Bu})](\text{PF}_6)_2$	24	R.T.	0.0012	[66]	43
9 ^[h]	$[\text{Fe}^{\text{II}}(\text{Cl}_3\text{TPAFeX}_2)(\text{OTf})_2]$	4.5	/	0.0023	[67]	3.9

^[a] $\text{H}_2\text{L}^1 = 2,3$ -dihydroxybenzylidene-2-hydroxybenzohydrazide.

^[b]Tp= tris (pyrazolyl) borate. ^[c]H₃tea= triethanolamine.

^[d]MeDea= N-methyldiethanolamine. ^[e]pz= pyrazol-1-yl.

^[f] $[\text{Fe}(\text{salhd})\text{Cl}] = \text{chloro-}[N,N'\text{-bis}(\text{salicylaldehyde})\text{-cyclohexanodiminate}] \text{ iron(III)}$.

^[g]NCCN= a tetradentate bis (pyridyl-N-heterocyclic carbene) ligand.

^[h] $\text{Cl}_n\text{TPAFeX}_2 = \text{a series of } \alpha\text{-chlorinated tripods in the tris (2-pyridylmethyl) amine series Cl}_n\text{TPA (n= 1-3) and fully characterized the corresponding FeX}_2 \text{ complexes (X= Cl, CF}_3\text{SO}_3\text{)}$.

The catalytic activity of complex **2** in Cy oxidation is also compared with other catalysts reported in the literature in **Table 5**. The total amount of CyOH+CyO produced by complex **2** is the highest one.

4. Conclusion

Three new complexes have been successfully synthesized by the reaction of $\text{MO}(\text{acac})_2$ with hydrazone or salicylaldehyde for the first time. All complexes are characterized by IR, UV and thermostability. The central metals are six-coordinate in the complexes and in an octahedral environment detected by single-crystal X-ray diffraction analyses. Their catalytic activities are studied in Cy oxidation using H_2O_2 as oxidant. The optimization of parameters, such as the concentration of oxidant, the type of solvent, the amount of acids, reaction temperature and the type of acids have been found. Interesting, Sebacic acid and FeCl_3 show positive effect on the oxidation with HNO_3 . The sequencing of the catalytic ability is complex $2 > 3 > 1$, due to the ability of ligands to release the active sites of central metal.

Supplementary material

CCDC reference numbers 1586416 for **1**, 1586417 for **2**, and 1586418 for **3** contain the supplementary crystallographic data for this article. These data can be obtained free of charge at <http://www.ccdc.cam.ac.uk>, or from Cambridge Crystallographic Data Center, 12 Union Road, Cambridge CB2 1EZ, UK; Fax: +44 1223 336 033; Email: deposit@ccdc.cam.ac.uk.

Acknowledgments

This work was financially supported by the support plan of high-level personnel innovation of Dalian [no. 2015R070], the Basic research project of Key Laboratory of Liaoning Province [no. LZ2015048], the Education Office of Liaoning Province [Project No. LF201783611] and the Innovative Entrepreneurial Training Program of Liaoning Normal University [Project No. cx201802017].

References

- [1] R. A. Sheldon, *Stud. Surf. Sci. Catal.* 66 (1991) 33.
- [2] M. D. Hughes, Y. J. Xu, P. Jenkins, P. McMorn, P. Landon, D. I. Enache, A. F. Carley, G. A. Attard, G. J. Hutchings, F. King, E. H. Stitt, P. Johnston, K. Griffin, C. J. Kiely, *Nature* 437 (2005) 1132.

- [3] C. L. Hill, I. A. Weinstock, *Nature* 401 (1999) 436.
- [4] W. Buijs, *Topics Catal.* 24 (2003) 73.
- [5] A. E. Shilov, G. B. Shul'pin, *Chem. Rev.* 97 (1997) 2879.
- [6] T. Wang, Y. She, H. Fu, H. Li, *Catalysis Today* 264 (2016) 185.
- [7] R.H. Crabtree, *Chem. Rev.* 95 (1995) 987.
- [8] D. Palomas, C. Kalamaras, P. Haycock, A. J. P. White, K. Hellgardt, A. Horton, M. R. Crimmin, *Catal. Sci. Technol.* 5 (2015) 4108.
- [9] M. M. Vinogradov, Y. N. Kozlov, D. S. Nesterov, L. S. Shul'pina, A. J. L. Pombeiro, G. B. Shul'pin, *Catal. Sci. Technol.* 4 (2014) 3214.
- [10] A. Pariyar, S. Bose, A. N. Biswas, S. Barman, P. Bandyopadhyay, *Catal. Sci. Technol.* 4 (2014) 3180.
- [11] G. Olivo, G. Arancio, L. Mandolini, O. Lanzalunga, S. Di Stefano, *Catal. Sci. Technol.* 4 (2014) 2900.
- [12] S. Hazra, A. P. C. Ribeiro, M. Fátima C. G. Da Silva, C. A. N. De Castro, A. J. L. Pombeiro, *Dalton Trans.* 45 (2016) 13957.
- [13] A. A. K. U. Ingold, K. U. Ingold, *Aldrichim. Acta.* 22 (1989) 1.
- [14] U. Schuchardt, D. Cardoso, R. Sercheli, R. Pereira, R. S. Da Cruz, M. C. Guerreiro, D. Mandelli, E. V. Spinacé, E. L. Pires, *Appl. Catal. A Gen.* 211 (2001) 1.
- [15] G. Sankar, R. Raja, J. M. Thomas, *Catalysis Letters* 55 (1998) 15.
- [16] G. Huang, L. Mo, J. Cai, X. Cao, Y. Peng, Y. Guo, S. Wei, *Applied Catalysis B: Environmental* 162 (2015) 364.
- [17] X. Song, J. Hao, Y. Bai, L. Han, G. Yan, X. Lian, J. Liu, *NewJ. Chem.* 41 (2017) 4031.
- [18] A. A. Alshaheri, M. I. M. Tahir, M. B. A. Rahman, T. B. S. A. Ravoof, T. A. Saleh, *Chem. Eng. J.* 327 (2017) 423.
- [19] K. Seo, H. Kim, J. Lee, M.G. Kim, S. Y. Seo, C. Kim, *Journal of Industrial and Engineering Chemistry* 53 (2017) 371.
- [20] P. C. A. Bruijninx, I. L. C. Buurmans, Y. Huang, G. Juhász, M. Viciano-Chumillas, M. Quesada, J. Reedijk, M. Lutz, A. L. Spek, E. Münck, E. L.

- Bominaar, R. J. M. K. Gebbink, *Inorg. Chem.* 50 (2011) 9243.
- [21] A. C. Lindhorst, S. Haslinger, F. E. Kühn, *Chem. Commun.* 51 (2015) 17193.
- [22] Luyan Li, Qihao Yang, Si Chen, Xudong Hou, Bo Liu, Junling Lu, Hai-Long Jiang, *Chem. Commun.* 53 (2017) 10026.
- [23] R. R. Mendel, *Metallomics and the Cell* 12 (2013) 503.
- [24] S. Huber, M. Cokoja, F. E. Kühn, *J. Organomet. Chem.* 751 (2014) 25.
- [25] C. J. Hinshaw, G. Peng, R. Singh, J. T. Spence, J. H. Enemark, M. Bruck, J. Kristofzski, S. L. Merbs, R. B. Ortega, P. A. Wexler, *Inorg. Chem.* 28 (1989) 4483.
- [26] R. D. Chakravarthy, D. K. Chand, *J. Chem. Sci.* 123 (2011) 187.
- [27] S. Etal, *Coord. Chem. Rev.* 95 (1989) 183.
- [28] D. Biswal, N. R. Pramanik, S. I. Chakrabarti, M. G. B. Drew, B. Sarkar, M. R. Maurya, S. K. Mukherjee, P. Chowdhury, *NewJ. Chem.* 41 (2017) 4116.
- [29] M. Bagherzadeh, M. Zare, V. Amani, A. Ellern, L. K. Woo, *Polyhedron* 53 (2013) 223.
- [30] A. C. Gomes, P. Neves, L. C. Silva, A. A. Valente, I. S. Gonçalves, M. Pillinger, *Catal. Sci. Technol.* 6 (2016) 5207.
- [31] A. A. Alshaheri, M. I. M. Tahir, M. B. A. Rahman, T. Begum, T. A. Saleh, *Journal of Molecular Liquids* 240 (2017) 486.
- [32] H. S. Hothi, M. Bhandari, J. R. Sharma, *Pesticide Research Journal* 12 (2000) 248.
- [33] S. Di. Bella, I. Fragalà, *NewJ. Chem.* 26 (2002) 285.
- [34] S. A. Aboafia, S. A. Elsayed, A. K. A. El-Sayed, A. M. El-Hendawy, *Journal of Molecular Structure* 1158 (2018) 39.
- [35] Bruker, SMART (Version 5.628) and SAINT (Version 6.02), Bruker AXS Inc., Madison, Wisconsin, USA, 1998.
- [36] G. M. Sheldrick, SADABS. Program for Empirical Absorption Correction of Area Detector, University of Göttingen, Germany, 1996.
- [37] G. M. Sheldrick, *Acta Crystallogr. A* 64 (2008) 112.
- [38] G. B. Shul'pin, *Journal of Molecular Catalysis A:Chemical* 189 (2002) 39.

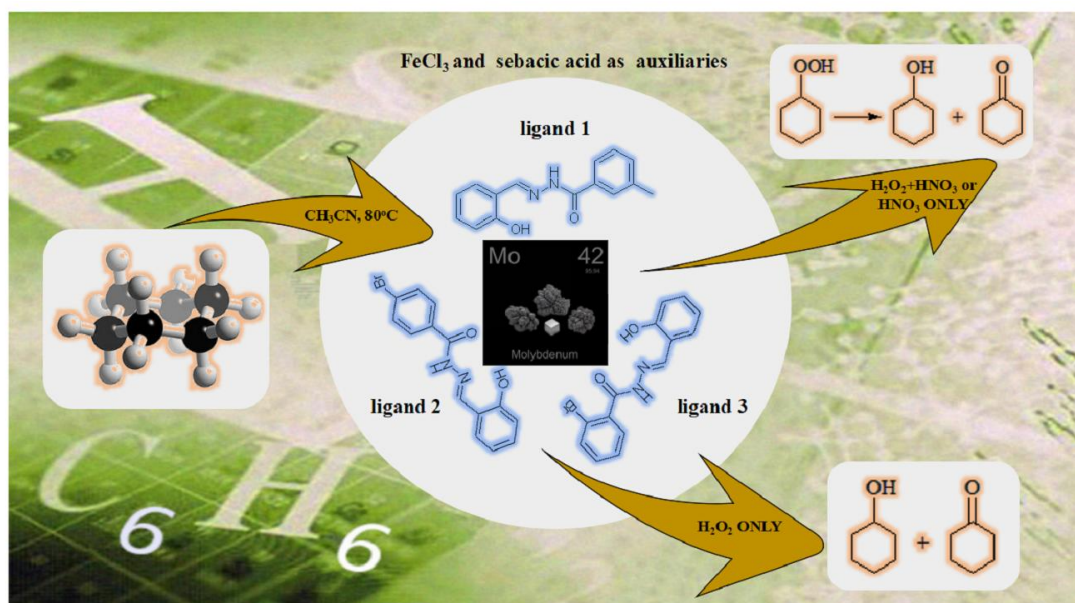
- [39] Y. L. Zhai, X. X. Xu, X. Wang, *Polyhedron* 11 (1992) 415.
- [40] R. Dinda, S. Ghosh, L. R. Falvello, M. Tomas, T. C. W. Mak, *Polyhedron* 25 (2006) 2375.
- [41] R. Dinda, S. Sengupta, S. Ghosh, H. Mayer-Figge, W. S. Sheldrick. *J. Chem. Soc. Dalton Trans.* 23 (2002) 4434.
- [42] S. Gupta, A. K. Barik, S. Pal, A. Hazra, S. Roy, R. J. Butcher, S. K. Kar, *Polyhedron* 26 (2007) 133.
- [43] W. Banße, E. Ludwig, U. Schilde, E. Uhlemann, F. Weller, A. Lehmann, *Z. Anorg. Allg. Chem.* 621 (1995) 1275.
- [44] S. Ghosh, T. K. Bandyopadhyay, P. K. Ray, M. S. Mitra, *J. Inorg. Biochem.* 20 (1984) 79.
- [45] N. S. Biradar, B. R. Havinale, *Inorg. Chim. Acta.* 17 (1976) 157.
- [46] M. R. Maurya, N. Saini, F. Avecilla, *RSC Adv.* 5 (2015) 101076.
- [47] M. E. Judmaier, C. Holzer, M. Volpe, N. C. Mösch-Zanetti, *Inorg. Chem.* 51 (2012) 9956.
- [48] D. Wang, M. Ebel, C. Schulzke, C. Grüning, S. K. S. Hazari, D. Rehder, *Eur. J. Inorg. Chem.* 4 (2001) 935.
- [49] J. C. Pessoa, M. J. Calhorda, I. Cavaco, I. Correia, M. T. Duarte, V. Felix, R. T. Henriques, M. F. M. Piedade, I. Tomaz, *J. Chem. Soc. Dalton Trans.* 23 (2002) 4407.
- [50] M. R. Maurya, N. Kumar, *Journal of Molecular Catalysis A: Chemical* 406 (2015) 204.
- [51] C. Zang, H. Tang, J. Wang, Y. Ge, Y. Shi, *Material & Heat Treatment* 37 (2008) 125.
- [52] Y. Marcus, J. Rydberg, C. Musikas, G. R. Choppin (Eds), *Principles and Practices of Solvent Extraction*, Marcel Dekker, New York, 1992, pp. 23.
- [53] S. Tang, J. She, Z. Fu, S. Zhang, Z. Tang, C. Zhang, Y. Liu, D. Yin, J. Li, *Applied Catalysis B: Environmental* 214 (2017) 89.
- [54] Q. Wu, N. Xing, X. Ma, L. Xu, Y. Xing, *Chinese Journal of Applied Chemistry* 32 (2015) 85.
- [55] M. Sutradhar, N. V. Shvydkiy, M. F. C. G. Da Silva, M. V. Kirillova, Y. N. Kozlov,

- A. J. L. Pombeiro, G. B. Shul'pin, Dalton Trans. 42 (2013) 11791.
- [56] A. Pokutsa, O. Fliunt, Y. Kubaj, T. Paczeński, P. Blonarz, R. Prystanskiy, J. Muzart, R. Makitra, A. Zaborovskiy, A. Sobkowiak, Journal of Molecular Catalysis A: Chemical 347 (2011) 15.
- [57] S. M. Yiu, W. L. Man, T. C. Lau, J. Am. Chem. Soc. 130 (2008) 10821.
- [58] C. M. Ho, T. C. Lau, New J. Chem. 24 (2000) 587.
- [59] Y. Du, Y. Xiong, J. Li, X. Yang, Journal of Molecular Catalysis A: Chemical 298 (2009) 12.
- [60] M. Sutradhar, A. P. C. Ribeiro, M. F. C. G. Da Silva, A. M. F. Palavra, A. J. L. Pombeiro, Molecular Catalysis 2017, in press, 10.1016/j.mcat.2017.10.026.
- [61] N. Xing, H. Shan, X. Tian, Q. Yao, L. Xu, Y. Xing, Zhan Shi, Dalton Trans. 42 (2013) 359.
- [62] Y. Y. Karabach, M. F. C. G. Da Silva, M. N. Kopylovich, B. Gil-Hernández, J. Sanchiz, A. M. Kirillov, A. J. L. Pombeiro, Inorg. Chem. 49 (2010) 11096.
- [63] D. S. Nesterov, V. N. Kokozay, J. Jezierska, O. V. Pavlyuk, R. Boča, A. J. L. Pombeiro, Inorg. Chem. 50 (2011) 4401.
- [64] L. M. D. R. S. Martins, M. P. De Almeida, S. A. C. Carabineiro, J. L. Figueiredo, A. J. L. Pombeiro, ChemCatChem 12 (2013) 3847.
- [65] A. R. Silva, T. Mourão, J. Rocha, Catalysis Today 203 (2013) 81.
- [66] S. Haslinger, A. Raba, M. Cokoja, A. Pöthig, F. E. Kühn, Journal of Catalysis 331 (2015) 147.
- [67] H. Jaafar, B. Vilen, A. Thibon, D. Mandon, Dalton Trans. 40 (2011) 92.

Highlights

- Three new dioxomolybdenum(VI) complexes are synthesized.
- These complexes are tested as catalysts for cyclohexane oxidation.
- Sebacic acid and FeCl_3 as acid auxiliaries are effective to promote the reaction.

ACCEPTED MANUSCRIPT



ACCEPTED MANUSCRIPT